

Original Research Article

UTILITY OF CT ATTENUATION VALUE IN DIFFERENTIATING ENOSTOSIS FROM UNTREATED OSTEOLASTIC METASTASES

K. Priyanka¹, Chaitanya Deep DSJ², O. Sridhar Babu³

¹Assistant Professor, Department of Radiodiagnosis, Sri Venkateswara Medical College, Tirupati, Andhra Pradesh, India.

²Assistant Professor, Department of Radiodiagnosis, Sri Venkateswara Medical College, Tirupati, Andhra Pradesh, India.

³Associate Professor, Department of Radiodiagnosis, Sri Venkateswara Medical College, Tirupati, Andhra Pradesh, India.

Received : 03/07/2025
Received in revised form : 18/08/2025
Accepted : 06/09/2025

Corresponding Author:

Dr. K. Priyanka,
Assistant Professor, Department of
Radiodiagnosis, Sri Venkateswara
Medical College, Tirupati, Andhra
Pradesh, India.
Email: priyankaobulampalli@gmail.com

DOI: 10.70034/ijmedph.2025.4.31

Source of Support: Nil,
Conflict of Interest: None declared

Int J Med Pub Health
2025; 15 (4); 170-174

ABSTRACT

Background: This study was conducted with an aim to assess the utility of CT attenuation values in differentiating enostosis from untreated osteoblastic metastases using mean and maximum Hounsfield Unit (HU) measurements.

Materials and Methods: This prospective observational study included 78 patients divided equally into two groups—enostosis and osteoblastic metastasis—based on clinical and radiologic criteria. CT examinations were performed using a 16-slice CT scanner (GE Revolution). For each lesion, four-quadrant ROI measurements were taken to calculate mean and maximum attenuation values. Statistical analysis included t-tests, chi-square tests, and ROC curve analysis to determine diagnostic performance.

Results: Mean CT attenuation was significantly higher in the enostosis group (1053.91 ± 73.59 HU) compared to the metastasis group (938.41 ± 56.96 HU) ($p < 0.001$). Similarly, maximum attenuation values were higher in enostosis (1171.41 ± 58.00 HU vs. 999.23 ± 56.69 HU, $p < 0.001$). ROC curve analysis demonstrated excellent diagnostic accuracy, with visually estimated AUCs exceeding 0.95 for both parameters. A cutoff of approximately 885 HU for mean and 1060 HU for maximum attenuation yielded high sensitivity and specificity, aligning with published literature.

Conclusion: CT-based attenuation values, especially the maximum and mean HU measurements, differentiate the enostosis from osteoblastic metastases. Incorporating these measurements into day-to-day CT interpretation aids in enhancing diagnostic accuracy.

Abbreviations: CT = Computed tomography, HU = Hounsfield units, ROC = receiver operating characteristics, AUC = Area under curve

Key words: Enostosis, Bone Island, Osteoblastic Metastasis, CT Attenuation, Hounsfield Unit, ROC Curve, Bone Lesions.

INTRODUCTION

Enostosis, commonly referred to as a bone island, is a benign, asymptomatic lesion composed of compact cortical bone embedded within the cancellous bone.^[1] These lesions are typically discovered incidentally on imaging studies, particularly CT scans, due to their radiodense appearance and predilection for sites such as the pelvis, femur, and vertebrae.^[2] Enostoses are characterized by their homogenous density and sharp, feathered margins blending with adjacent trabeculae, which help in distinguishing them from pathological entities on imaging modalities like radiography and

CT scans.^[3] However, the increasing use of cross-sectional imaging has led to more frequent incidental detection of such sclerotic lesions, raising diagnostic dilemmas, particularly in oncology patients where osteoblastic bone metastases are a significant concern.^[4]

Osteoblastic metastases, which originate from primary malignancies such as those of the prostate, breast, or lung, often present as sclerotic lesions and can closely mimic enostoses on CT imaging.^[5] Accurate differentiation is crucial, as mistaking a metastatic lesion for a benign bone island—or vice versa—could significantly impact staging, treatment

decisions, and prognosis.^[6] Recent literature highlights the potential of quantitative CT attenuation (measured in Hounsfield Units) in distinguishing between these entities.^[7,8] Ulano et al. demonstrated that a mean attenuation below 885 HU and a maximum below 1060 HU favors the diagnosis of metastasis, offering high sensitivity and specificity in differentiating the two. Despite this, such objective thresholds are underutilised in routine practice, and literature on their practical application remains limited, prompting the need for further validation through prospective observational studies like the present one.

Aim

1. To differentiate Osteoblastic metastases from bone islands using CT attenuation value.

Objectives

1. Characterisation of enostoses
2. Characterisation of osteoblastic metastases

MATERIALS AND METHODS

Study Design and Setting

This prospective observational study was conducted in the Department of Radiodiagnosis at Sri Venkateswara Medical College and SVRRGGH, Tirupati, Andhra Pradesh, India. The study was conducted for a period of 3 months after approval from the institute ethical committee.

Study Population

This study considered a sample size of 78, which was equally divided between the two groups. The enostosis Group (n=39) had incidentally detected benign bone islands on thoracic and abdominal CT without any history of malignancy. The other group, osteoblastic metastasis (n=39), contains the patients with the known malignancy and confirmed radiological osteoblastic lesions, later supported by the clinical and histopathological studies.

Inclusion Criteria

- Adults aged 20–90 years.
- **Enostosis group:** Patients without prior or known malignancy.
- **Metastasis group:** Patients with untreated, histologically or radiologically confirmed osteoblastic skeletal metastases.

Exclusion Criteria

- Patients with prior chemotherapy or radiotherapy.
- Poor-quality or incomplete CT data.
- Pediatric patients or those outside the defined age range.

Methodology of the study

All CT scans were performed on a 16-slice GE Revolution scanner with a slice thickness of 5 mm and a tube voltage of 120 kVp. Coronal and sagittal reconstructions were generated at 2 mm intervals for detailed evaluation. For each identified lesion, four region-of-interest (ROI) measurements were

obtained in orthogonal quadrants, carefully avoiding cortical bone and sclerotic margins. The ROI area was approximately 1 mm². Quantitative analysis included the mean attenuation value (Hounsfield Units, HU), calculated as the average of the four readings, and the maximum attenuation value (HU), defined as the highest single measurement within the lesion.

Data Collection and Statistical Analysis

All data were recorded in Microsoft Excel and analysed using statistical software SPSS V.29.0. Descriptive statistics were expressed as mean \pm standard deviation for quantitative variables. Comparative analysis between the two groups was performed using the independent sample t-test for attenuation values and the chi-square test for categorical variables such as age group, sex, and lesion site. Diagnostic performance was assessed using receiver operating characteristic (ROC) analysis to identify optimal HU thresholds and to calculate sensitivity, specificity, and the area under the curve (AUC) for both mean and maximum attenuation values.

Ethical Considerations

The study was approved by the Institutional Ethics Committee of S.V. Medical College, Tirupati. Written informed consent was obtained from all participants. Patient confidentiality and anonymity were strictly maintained throughout the study.

RESULTS

The current study utilised computed tomography-based attenuated values to differentiate osteoblastic metastasis from enostosis with a sample size of 78 patients equally divided between the two groups. The demographic distribution between the two groups has shown a statistically significant difference with the p-value of 0.001. [Table 1 and Table 2] Enostosis was commonly found in the vertebral bodies and long bones, whereas the osteoblastic metastasis was found frequently in the ribs, scapula and posterior elements. [Table 3]

The enostosis group showed the mean (Table 4) and maximum attenuation (Table 5) values (1053.91 ± 73.59 HU and 1171.41 ± 58.00 HU, respectively) comparably higher than the osteoblastic metastasis group (938.41 ± 56.96 HU and 999.23 ± 56.69 HU), which is statistically significant with a p-value of <0.001 for both parameters of mean and maximum attenuation. ROC curve demonstrated excellent diagnostic accuracy with a curve of mean and maximum attenuation approaching the near-perfect difference between the two groups (Visual AUC estimate: 0.96-0.99). This study's findings support the usage of CT attenuation, especially maximum HU values, as a non-invasive and reliable marker to differentiate enostosis from osteoblastic metastasis in clinical practice.

Table 1: Distribution of age between the study groups

Age (Years)	Group		Total	P-value(chi-square test)
	Enostosis	Osteoblastic Metastasis		
<=45	12	4	16	0.001
46 - 60	14	5	19	
61 & Above	13	30	43	
Total	39	39	78	

Table 2: Distribution of the gender between the study groups

Sex	Group		Total	P-value (chi-square test)
	Enostosis	Osteoblastic Metastasis		
Male	34	20	54	0.001
Female	5	19	24	
Total	39	39	78	

Table 3: Association between the bone site of the lesions and the groups

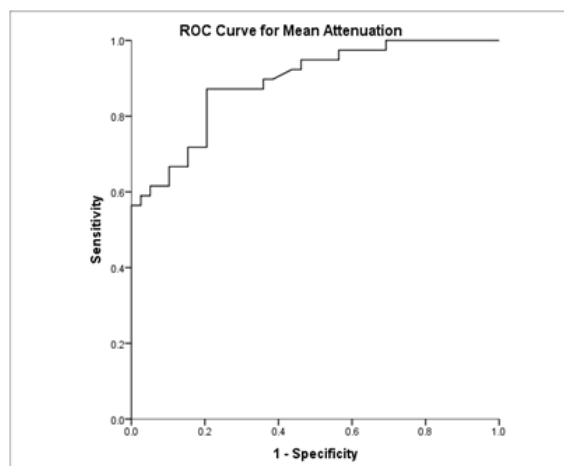
Bone Site	Group		Total	P-value (chi-square test)
	Enostosis	Osteoblastic Metastasis		
Clavicle	1	0	1	0.013
Femur	9	5	14	
Humerus	5	0	5	
Pelvic Bones	6	8	14	
Posterior Elements	3	5	8	
Ribs	0	5	5	
Scapula	0	5	5	
Sternum	1	2	3	
Vertebral Body	14	9	23	
Total	39	39	78	

Table 4: Comparison of the mean attenuation HU value between the groups

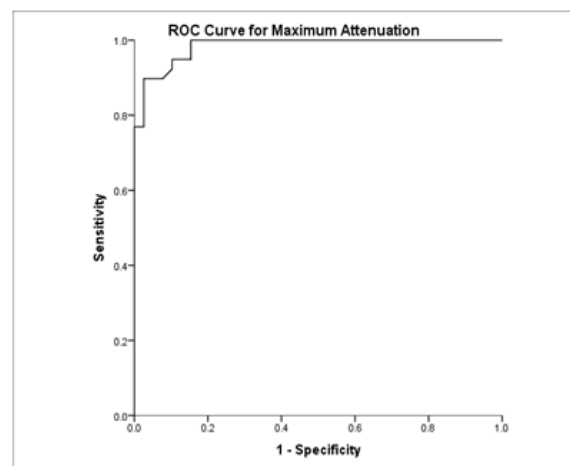
Group	Mean Attenuation		P Value (t-test)
	Mean	Std. Deviation	
Enostosis	1053.91	73.593	<0.001
Osteoblastic Metastasis	938.41	56.962	

Table 5: Comparison of the maximum attenuation HU value between the groups

Group	Maximum Attenuation		P Value (t-test)
	Mean	Std. Deviation	
Enostosis	1171.41	58.002	<0.001
Osteoblastic Metastasis	999.23	56.691	

**Figure 1: ROC curve for the mean attenuation**

Cut off Value	975.5
Sensitivity	87.2%
Specificity	79.5%

**Figure 2: ROC curve for the maximum attenuation**

Cut off Value	1098
Sensitivity	89.7%
Specificity	97.4%



Figure 3: Axial image of CT abdomen showing the sclerotic focus in T11 vertebral body consistent with enostosis

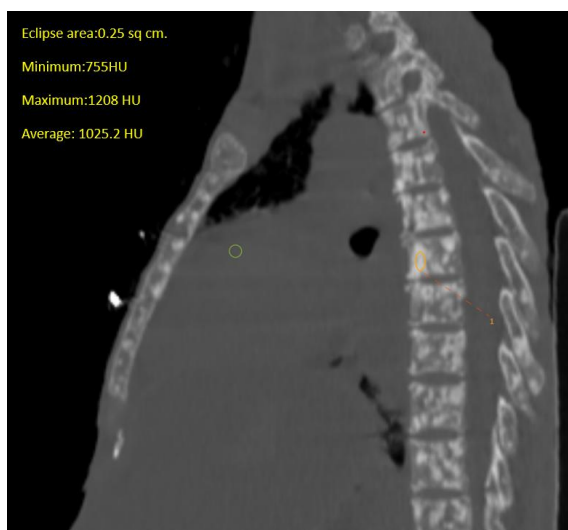


Figure 4: Sagittal image of CT Thorax showing the metastatic focus in T5 vertebral body consistent with osteoblastic metastasis in a case of metastatic breast carcinoma

DISCUSSION

In modern clinical practice, it is essential to differentiate benign enostosis from osteoblastic metastasis to avoid misclassification of bone lesions, thereby preventing inappropriate staging and treatment. Earlier, conventional features like sclerotic margins and feathered margins were used to differentiate these less accurate lesions, but with the advent of computed tomography, the task has been made easier using the HU values.^[9,10] In this study, we used this attenuation value to establish the range of HU values to distinguish between these two lesions.

This study's results revealed in the enostosis group, the mean attenuation value of 1053.91 HU and maximum attenuation value of 1171.41 HU are

significantly higher than of the osteoblastic metastases group with mean attenuation value of 938.41HU and maximum attenuation value of 999.23 HU. The p-value value for this comparison was <0.001 which was statistically significant. These findings were in consistent with study conducted by Ulano et al,^[11] in which 279 sclerotic lesions and reported mean and maximum CT attenuation values of 1190 ± 239 HU and 1323 ± 234 HU for enostoses, and 654 ± 176 HU and 787 ± 194 HU for metastases, respectively. Their study established the cut-off values of 885HU for the mean and 1060HU for the maximum attenuation, achieving an AUC of 0.982 with 95% sensitivity and 96% specificity. In another study by Sala et al,^[12] found that the incidental bone islands and untreated osteoblastic metastases, demonstrating a high discriminative accuracy with an AUC of 0.982, using a mean attenuation cutoff of 881 HU. Their findings showed enostosis HU values range from 1007 ± 122 HU to 1052 ± 107 HU, further validating our data.

Supporting with additional insights from Elangovan and Sebro,^[13] who evaluated both treated and untreated metastases in their cohort of 165 patients. They revealed the significantly lower attenuation in both groups of metastases (mean HU: 602 untreated and 731.7 treated) than in enostoses (1123 HU). Their study results reinforced that CT attenuation thresholds (885 HU for mean, 1060 HU for maximum) maintain high diagnostic accuracy for untreated metastases (91.7%) but are slightly reduced for treated lesions (81.7%). These results confirm that prior therapy can confound attenuation-based diagnosis and should be considered in the clinical context.

In line with evolving imaging techniques, Xu et al,^[14] explored the role of dual-energy CT (DECT) metrics in a cohort of 110 patients. Parameters such as effective atomic number (Z_{mean}), dual energy index (DEI), and electron density (ρ) demonstrated superior diagnostic performance, with Z_{mean} showing an AUC of 0.91, sensitivity of 91.2%, and specificity of 82.5%. Although promising, these advanced DECT-based methods are not yet widely accessible in all centres, especially in resource-limited settings.

More recently, Ji-Hyung Hong et al,^[15] incorporated radiomics and machine learning into CT-based lesion classification. Using a random forest model trained on radiomic features, their external test set showed an AUC of 0.96, outperforming one of the three experienced radiologists. While radiomics adds a layer of diagnostic accuracy, it requires specialised software and computational expertise, making CT attenuation-based thresholds a more universally applicable and practical tool in most radiology departments.

This study further strengthens the utility of attenuation thresholds as a simple, reproducible, and widely accessible tool in differentiating enostoses from osteoblastic metastases. The ROC curve analysis in our study also revealed high diagnostic

performance, with AUCs visually approaching those reported in prior studies. Additionally, the significant demographic differences observed—osteoblastic metastases were more frequent in older individuals and females—align with known epidemiologic patterns and add context to imaging findings.

CONCLUSION

This prospective observational study results are aligned with existing evidence of that CT attenuation values, especially when assessed with clinical and anatomical integration, yield a high degree of diagnostic value in differentiating osteoblastic metastasis from enostosis. This study's findings support the utilisation of the quantitative HU thresholds in to routine radiological practice, especially in cases with a diagnostic dilemma.

REFERENCES

1. Falk GL, Simpson SB. Incidental benign skeletal lesions: bone islands. In: Clinical Atlas of Bone SPECT/CT. 2024 Jan 1. p. 783–7.
2. Quattrocchi CC, Santini D, Dell'Aia P, Piciucchi S, Leoncini E, Vincenzi B, et al. A prospective analysis of CT density measurements of bone metastases after treatment with zoledronic acid. *Skeletal Radiol.* 2007 Dec 3;36(12):1121–7.
3. Cerase A, Priolo F. Skeletal benign bone-forming lesions. *Eur J Radiol.* 1998 May 1;27(Suppl 1): S91–7.
4. Wang R, Zhou R, Sun S, Yang Z, Chen H. Histograms of computed tomography values in differential diagnosis of benign and malignant osteogenic lesions. *Acta Radiol.* 2024 Jun 1;65(6):625–31.
5. Vanhoenacker FM, Al-Musaedi A. Bone island. *Med Radiol.* 2024; Part F2937:167–77.
6. Li J, Cai L, Jiang N, Liu J. Differentiation of osteoblastic metastases and bone islands on dual-energy computed tomography in patients with untreated lung cancer. *Eur J Radiol.* 2024 Dec 1; 181:110355.
7. Greenspan A. Bone island (enostosis): current concept – a review. *Skeletal Radiol.* 1995;24(2):111–5.
8. Greenspan A. Benign spotted bones: a diagnostic dilemma. *CMAJ.* 2011;183(4):456–9.
9. Tang SZ, Hallinan JTPD, Sinha AK, Eide SE. Imaging in bone and soft tissue tumours. In: Clinical Management of Bone and Soft Tissue Tumors. 2025. p. 11–31.
10. Matcuk GR, Waldman LE, Fields BKK, Colangeli M, Palmas M, Righi A, et al. Conventional radiography for the assessment of focal bone lesions of the appendicular skeleton: fundamental concepts in the modern imaging era. *Skeletal Radiol.* 2025 Jul 1;54(7):1391–406.
11. Ulano A, Bredella MA, Burke P, Chebib I, Simeone FJ, Huang AJ, et al. Distinguishing untreated osteoblastic metastases from enostoses using CT attenuation measurements. *AJR Am J Roentgenol.* 2016 Aug 1;207(2):362–8.
12. Sala F, Dapoto A, Morzenti C, Firetto MC, Valle C, Tomasoni A, et al. Bone islands incidentally detected on computed tomography: frequency of enostosis and differentiation from untreated osteoblastic metastases based on CT attenuation value. *Br J Radiol.* 2019 Nov 1;92(1103):20190249.
13. Elangovan SM, Sebro R. Accuracy of CT attenuation measurement for differentiating treated osteoblastic metastases from enostoses. *AJR Am J Roentgenol.* 2018 Mar 1;210(3):615–20.
14. Xu C, Kong L, Deng X. Dual-energy computed tomography for differentiation between osteoblastic metastases and bone islands. *Front Oncol.* 2022 Jul 12; 12:815955.
15. Hong JH, Jung JY, Jo A, Nam Y, Pak S, Lee SY, et al. Development and validation of a radiomics model for differentiating bone islands and osteoblastic bone metastases at abdominal CT. *Radiology.* 2021 Jun 1;299(3):626–32.